

Received: 2019.09.01
Accepted: 2019.10.03
Published: 2019.11.18

A Novel Nanofiber Hydrogel Loaded with Platelet-Rich Plasma Promotes Wound Healing Through Enhancing the Survival of Fibroblasts

Authors' Contribution:
Study Design A
Data Collection B
Statistical Analysis C
Data Interpretation D
Manuscript Preparation E
Literature Search F
Funds Collection G

AB 1 **Peng Zhang**
CD 2 **Long Zhou**
DEF 2 **Lei Wang**
ABG 1 **Qirong Dong**

1 Department of Orthopedics, Second Affiliated Hospital of Soochow University, Suzhou, Jiangsu, P.R. China
2 Department of Orthopedics, Suzhou Science and Technology Town Hospital, The Affiliated Suzhou Science and Technology Town Hospital of Nanjing Medical University, Suzhou, Jiangsu, P.R. China

Corresponding Author: Qirong Dong, e-mail: dongqirong@suda.edu.cn

Source of support: This work was supported by Key Projects of Medical Science and Technology Program in Suzhou High-tech Zone (2018Z009)

Background: Hydrogels are ideal biological carriers *in vivo* and have been widely used in the treatment of wound healing through loading with or without bioactive substances. Platelet-rich plasma (PRP) is purified from autologous plasma and has known curative efficacy for wound healing. The combined efficacy of shorten poly-N-acetyl glucosamine (sNAG) hydrogels and PRP in the treatment of wound healing has not been previously assessed.

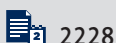
Material/Methods: The cytotoxic and proliferative effects of PRP on fibroblasts were detected using Cell Counting Kit-8 assays and flow cytometry. The levels of cyclin D1 and cyclin D3 were assessed to evaluate cell proliferation. Protein expression was assessed by western blot analysis. Adenosine levels were assessed by enzyme-linked immunosorbent assay. Cell apoptosis was assessed by flow cytometry and western blot analysis. Rat wound models were performed, and the effects of PRP, single hydrogels, and sNAG hydrogels loaded with PRP were respectively detected through the assessment of wound closure. Hematoxylin eosin staining was used to measure the depth and width of regenerative scars.

Results: Our results demonstrated that PRP promotes fibroblast proliferation and inhibits apoptosis. PRP contains abundant levels of adenosine, which has a positive role on fibroblast function, whilst the inhibition of adenosine A2A receptors impairs the efficacy of PRP. sNAG hydrogels loaded with PRP showed curative efficacy during wound healing in mice. Mice treated with hydrogels loaded with PRP showed high levels of regeneration with scarless healing.

Conclusions: Our results indicate that sNAG hydrogels loaded with PRP promote wound healing. The pro-proliferative, and anti-apoptotic effects of the fibroblasts are mediated by the activating A2A receptor in response to elevated adenosine levels.

MeSH Keywords: **Apoptosis • Cell Proliferation • Fibroblasts • Hydrogel Platelet-Rich Plasma**

Full-text PDF: <https://www.medscimonit.com/abstract/index/idArt/919812>



2228



7



23



Background

Wound healing is a complex pathophysiological process involving numerous cytokines, growth factors, chemokines, and cells; it includes 3 main stages: inflammation, proliferation, and tissue remodeling. During these processes, variations in the cellular and molecular environment can lead to chronic wound or scar formation [1]. Chronic wounds are often accompanied by other diseases [2] and up to 1% to 2% of the global population in the developed world will develop chronic wounds in their lifetime [3]. With the aging population, the occurrence of chronic wounds is anticipated to rise [4]. Chronic wounds cause pain and promote limb dysfunction and adverse emotions such as depression, anxiety, and tension. This imposes a heavy economic burden to patients and their families and exhausts medical resources [5].

PRP is a platelet-rich plasma obtained from the whole blood of human or animals after repeated centrifugation, that is rich in cells and growth factors, such as fibroblasts growth factors, platelet-derived factors, transformed growth factor beta, and vascular endothelial cell growth factor [6]. PRP has good therapeutic effects in wound healing, tissue repair and reconstruction [7]. A variety of cytokines and growth factors enriched in PRP regulate gene expression by activating cell surface receptors thereby regulating cell proliferation and apoptosis, participating in matrix degradation and tissue reconstruction in the wound [8]. These cytokines further promote angiogenesis within the wound, which provides a blood supply and nutrients for wound repair. Accumulating evidence have shown that platelet-rich plasma effectively stimulates angiogenesis [9], as well as relieving neuropathic scar pain at the wound surface [10].

Self-assembling peptide nanofiber materials (self-assembling peptide nanofiber scaffold, SAPNS) is one of the new achievements in the area of biological materials, which could absorb a lot of moisture and insoluble 3-dimensional polymer hydrogel. Due to its material-cell interface compatibility and good biological activity, it is considered an ideal repairing matrix material [11,12]. Previous studies have shown that SAPNS hydrogels can be loaded with antimicrobial peptides to accelerate chronic wound healing *in vitro* and *in vivo* [13,14]. Shorten poly-N-acetyl glucosamine (sNAG) nanofibers had been used for the treatment of chronic wound due to its advantage of promoting cell proliferation and migration and inducing the release of growth factors. However, research on the curative effects of sNAG combined with PRP in the treatment of wounds is sparse. In this study, we investigated the effect of sNAG hydrogels loaded with PRP on wound healing and explored its underlying mechanism.

Material and Methods

Cell culture

Fibroblasts were purchased from the Cell Bank of the Wuhan University, Wuhan, China. Cells were cultured in DMEM/F-12 (#10565042, ThermoFisher Scientific, GI, USA) containing 10% fetal bovine serum (FBS; #10099141, ThermoFisher Scientific, GI, USA).

Cell Counting Kit-8 (CCK-8) assays

Fibroblasts were seed into 96 well plates for 24, 48, or 72 hours and CCK-8 reagent was added to the cells in serum-free media for 2 hours. Cell viability was assessed by measurements of absorbance at 450 nm.

Flow cytometry

Propidium iodide (PI) staining was used for cell cycle progression assessments. Apoptosis was assessed using Annexin V-FITC/PI apoptosis detection kits (Genechem, Shanghai, China). For both approach cells were stained according to provided instructions and measured via flow cytometry.

Quantitative real-time polymerase chain reaction (qRT-PCR)

TRIzol (#15596018, Invitrogen, GI, USA) was used for RNA extraction according to manufacture protocols. A one-step Prime Script cDNA synthesis kit (Invitrogen, GI, USA) was used to produce cDNA. After which SYBR Premix Ex TaqII (#RR820A, TaKaRa, Japan) was used for amplification of equivalent cDNA amounts. A Thermal Cycler C-1000 Touch system (#10021377, Bio-Rad CFX Manager, USA) was used to perform qPCR analysis with GAPDH mRNA used for normalization. Data were given as fold change over appropriate controls. All primer sequences are as follows:

rat cyclin D1, 5'-GTCTTCCCCTGGCCATGAAGTAC-3' and

5'-AAGAAAGTGCCTTGTGCGGTAGCA-3';

rat cyclin D3, 5'-CAGTGACCGGACGGCTTGTG-3' and

5'-CACTTCAGTGCCTGTGATCC-3';

rat Bcl-2, 5'-TTTGAGTTCG GTGGGTCAT-3' and

5'-TGACTTCACT TGTGGCCAG-3';

rat Bax, 5'-TGGCAGCTGACATGTTTCTGAC-3' and

5'-TACCCAACACCTGGTCTT-3';

GAPDH, 5'-CCTCCGCTTCGCTCTCT-3' and

5'-CCGTTGACTCCGACCTTAC-3'.

Western blot

Tissues or cells were lysed via a lysis buffer (#AS1004, Aspen, South Africa) with 1% protease inhibitor (#AS1008, Aspen,

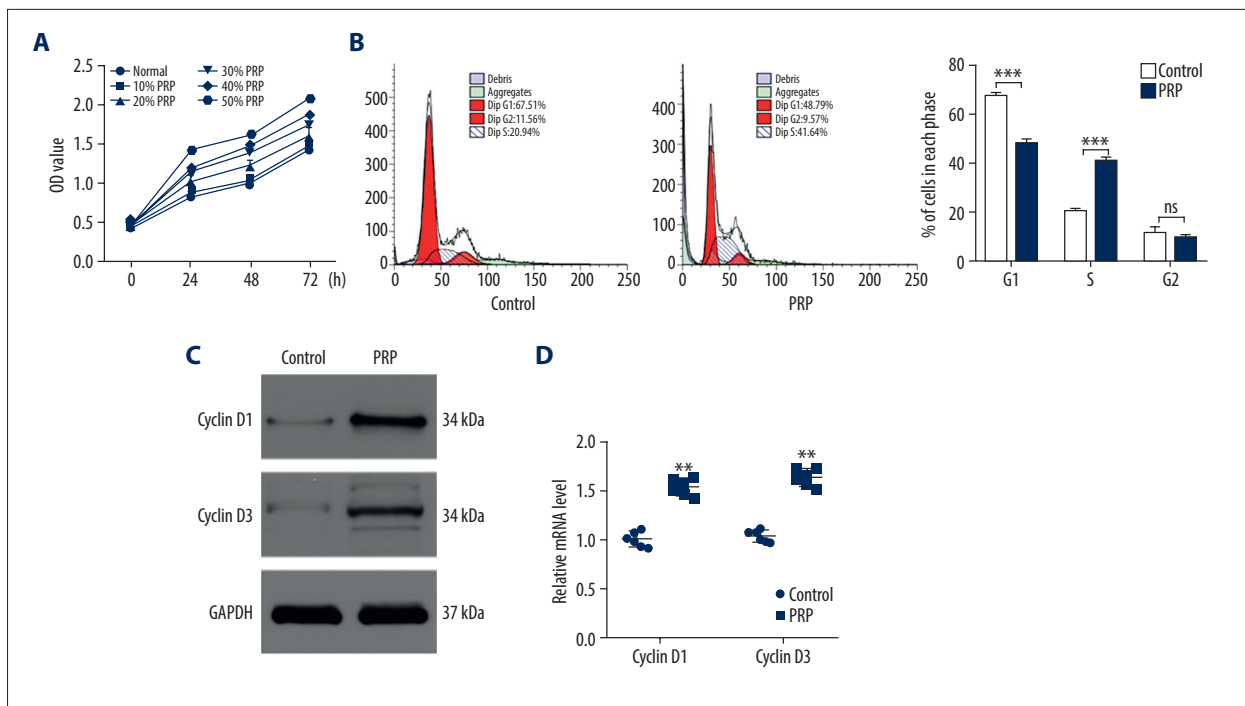


Figure 1. PRP promotes fibroblast proliferation *in vitro*. (A) The proliferation of fibroblasts among the 6 groups was measured by CCK-8. (B) Flow cytometry was used to assess the stage of cells. (C) The levels of cyclin D1 and cyclin D3 were measured by western blot analysis. (D) qRT-PCR analysis was applied to detect the expression of cyclin D1 and cyclin D3 in control and PRP groups. * $P < 0.05$, **** $P < 0.0001$. PRP – platelet-rich plasma CCK-8 – Cell Counting Kit-8; qR-PCR – quantitative real-time polymerase chain reaction.

South Africa) on ice. First, the protein fractions were collected, after which SDS-PAGE separation was carried out, followed by transfer onto a NC membrane (#IPVH00010, Millipore, USA). And then membranes were blocked by using 5% skim milk and probed at 4°C overnight, followed by HRP-conjugated secondary antibodies (#AS1058, Aspen, South Africa). Protein was visualized using a chemiluminescence detection system (#LiDE110, Canon, Japan). Antibodies were as follows: anti-Bcl-2 (#MAB-8272, 1: 500, R&D System, USA), anti-Bax (#AF820, 1: 1000, R&D System, USA), anti-cyclin D1 (#AF4196, 1: 500, R&D System, USA), and anti-cyclin D3 (#MAB6570, 1: 500, R&D System, USA). All experiments were conducted in triplicate.

Enzyme-linked immunosorbent assay (ELISA)

Normal serum and PRP was obtained from healthy volunteers, and the level of adenosine was measured by an ELISA kit (Abcam, UK).

Prepare of sNAG nanofibers hydrogels and PRP

To obtain the sNAG nanofibers, we used γ irradiated radiation to reduce N-acetylglucosamine fibers to formed shortened poly-N-acetylglucosamine fibers. Hydrogel sheets-based sNAG nanofibers was engineered as 1 cm in diameter. The PRP-loaded

sNAG hydrogels were prepared by adding PRP in sNAG hydrogel. Briefly, a total of 300 μ L of PRP solution was dropped on the hydrogel and incubated for 1 hour until PRP was absorbed.

Prepare of platelet-rich plasma

We obtained 5 mL of whole blood from healthy volunteers using a syringe containing 0.1 mL of acid dextrose anticoagulant agent (ACD-A), subsequently centrifuged at 1560 g for 10 minutes. Then, the supernatant was collected and centrifuged for a second time at 2340 g for 10 minutes.

Rat wound model and treatment

Male Sprague Dawley rats (200 g weight) were obtained from the center of experimental animals, Soochow University. Intraperitoneal pentobarbital sodium (50 mg/kg; Sigma-Aldrich, MO, USA) were used to anesthetize animals, after which the rat fur was shaved, and 1x1 cm full-thickness excision skin wounds were generated on the dorsum. The animals were divided into 4 groups according to the treatment method, including control (phosphate-buffered saline [PBS]), PRP, sNAG hydrogel, and PRP+sNAG hydrogel groups. For the PBS and PRP group, we injected 100 μ L of PBS or PRP around the wound site. For the other 2 groups, the hydrogel sheets were applied to cover

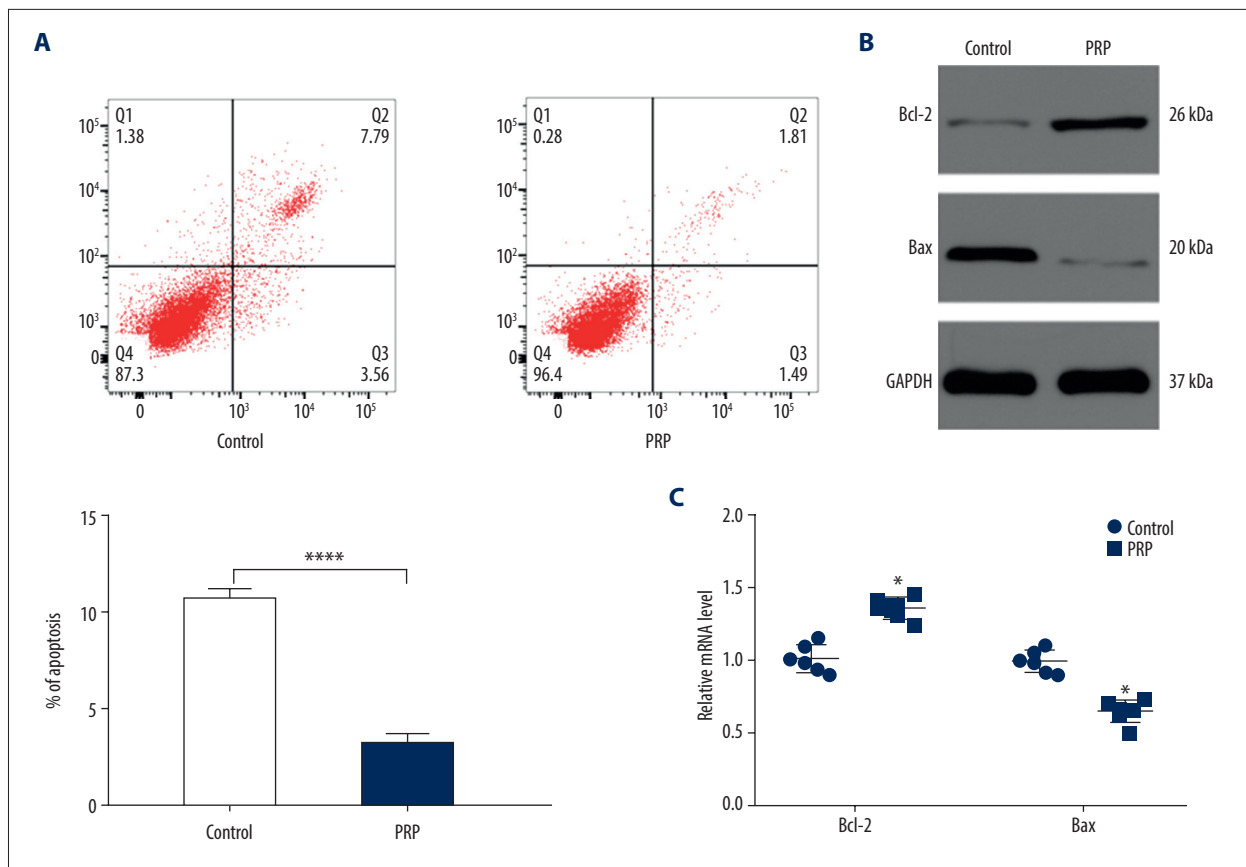


Figure 2. PRP suppress fibroblast apoptosis *in vitro*. (A) The apoptosis rate of fibroblasts among the 6 groups was measured by flow cytometry. (B) The levels of Bcl-2 and Bax were measured by western blot analysis. (C) qRT-PCR analysis was applied to detect the expression of Bcl-2 and Bax in control and PRP groups. * $P < 0.05$, **** $P < 0.0001$. PRP – platelet-rich plasma; qR-PCR – quantitative real-time polymerase chain reaction.

all wounds. The transparent dressing (Tegaderm™ film) was used to prevent damage to the wound. The Institution Animal Care and Use Committee of the Soochow University approved all animal studies (No. 2019-023-16).

Histological analysis

Skin samples were decalcified to obtain paraffin-embedded sections with a thickness of 5 to 7 μm . Samples were stained with hematoxylin-eosin (H&E). Immunofluorescence (IF) staining was performed as described [15].

Observation of wound closure

Wound closure rates were measured using digital images and quantified using ImageJ (National Institutes of Health) on days 0, 3, 5, 7, and 10. On day 14 post-injury, rats were euthanized, and wound tissues were paraffin embedded. H&E staining was performed, and samples were visualized (100 \times) to determine wound regeneration. Besides, the Ki67 staining was used to assess the proliferation of fibroblasts.

Statistical analysis

Data are the mean \pm standard deviation (SD). GraphPad Prism 7.0 (GraphPad Software, Inc., La Jolla, CA, USA) was used for all analyses. Three or more groups were measured through the one-way analysis of variance (ANOVA) with Tukey's post-hoc test. The 2-tailed Student's *t*-test was used for data comparison between the groups. $P < 0.05$ was deemed statistically significant.

Results

PRP induce fibroblasts proliferation *in vitro*

To explore the effects of PRP on fibroblasts, we performed CCK-8 assays to identify the optimal concentration of PRP for cell proliferation. Our data showed that PRP significantly promoted cell proliferation in a concentration-dependent manner (Figure 1A). We selected 50% PRP for subsequent experiments. Upon the assessment of cell cycle progression in the fibroblasts, a higher percentage of cells were arrested in the

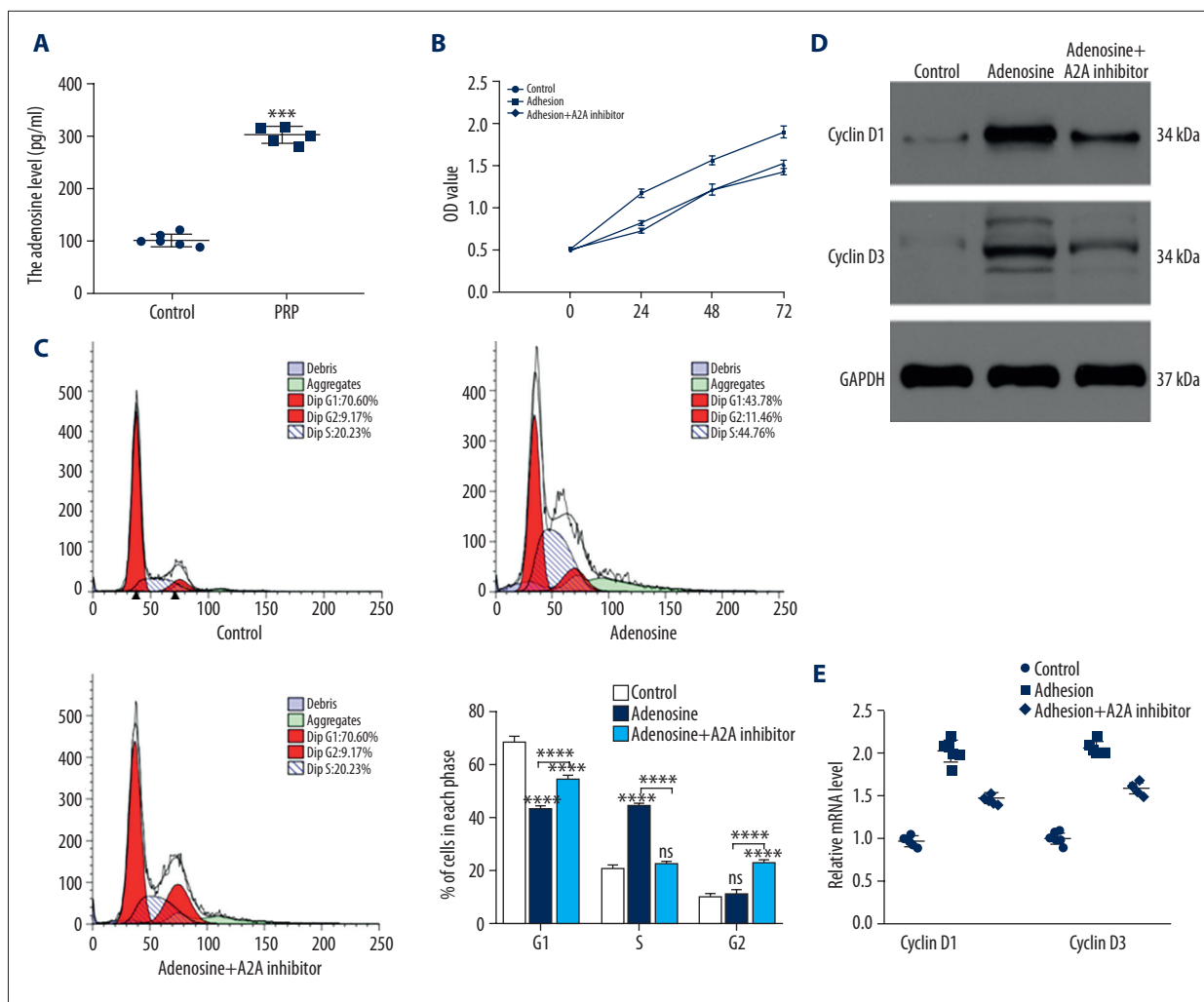


Figure 3. Adenosine is involved in PRP-induced cells proliferation. (A) The levels of adenosine in normal serum and PRP assessed by ELISA (n=6). (B, C) Fibroblasts were divided into 3 groups based on the different treatments. The proliferation of fibroblasts among the 3 groups was measured by CCK-8 and flow cytometry. (D) The levels of cyclin D1 and cyclin D3 were measured by western blot analysis. (E) qRT-PCR analysis was applied to detect the expression of cyclin D1 and cyclin D3 in control and PRP groups. PRP – platelet-rich plasma; ELISA – enzyme-linked immunosorbent assay; CCK-8 – Cell Counting Kit-8; qR-PCR – quantitative real-time polymerase chain reaction.

G1 stage of the cell cycle in the control group. In contrast, a higher proportion of cells entered the S stage in the PRP group (Figure 1B). Moreover, the proliferation-related genes cyclin D1 and cyclin D3 were detected via western blot (Figure 1C) and qRT-PCR analysis (Figure 1D). These results were consistent with flow cytometry assessments, highlighting the ability of PRP to induce fibroblast proliferation.

Fibroblasts apoptosis is suppressed by PRP

To investigate the effects of PRP on the apoptosis of fibroblasts, flow cytometry was performed. In cells treated with 50% PRP, the number of apoptotic cells were lower than other groups (Figure 2A). The levels of Bax and Bcl-2 were detected

by western blot analysis and qRT-PCR. As shown in Figure 2B and Figure 2C, PRP significantly reduced Bax expression and enhanced Bcl-2 expression compared to the control group. These data suggest that PRP suppresses fibroblast apoptosis.

Adenosine promotes fibroblast survival via A2A receptor activation

To detect the levels of adenosine in both normal serum and PRP, we collected 12 serum samples including 6 normal samples and 6 PRP samples. The levels of adenosine were measured by ELISA. As shown in Figure 3A, higher level of adenosine was observed in the PRP group compared to normal samples. To investigate the role of adenosine on fibroblasts,

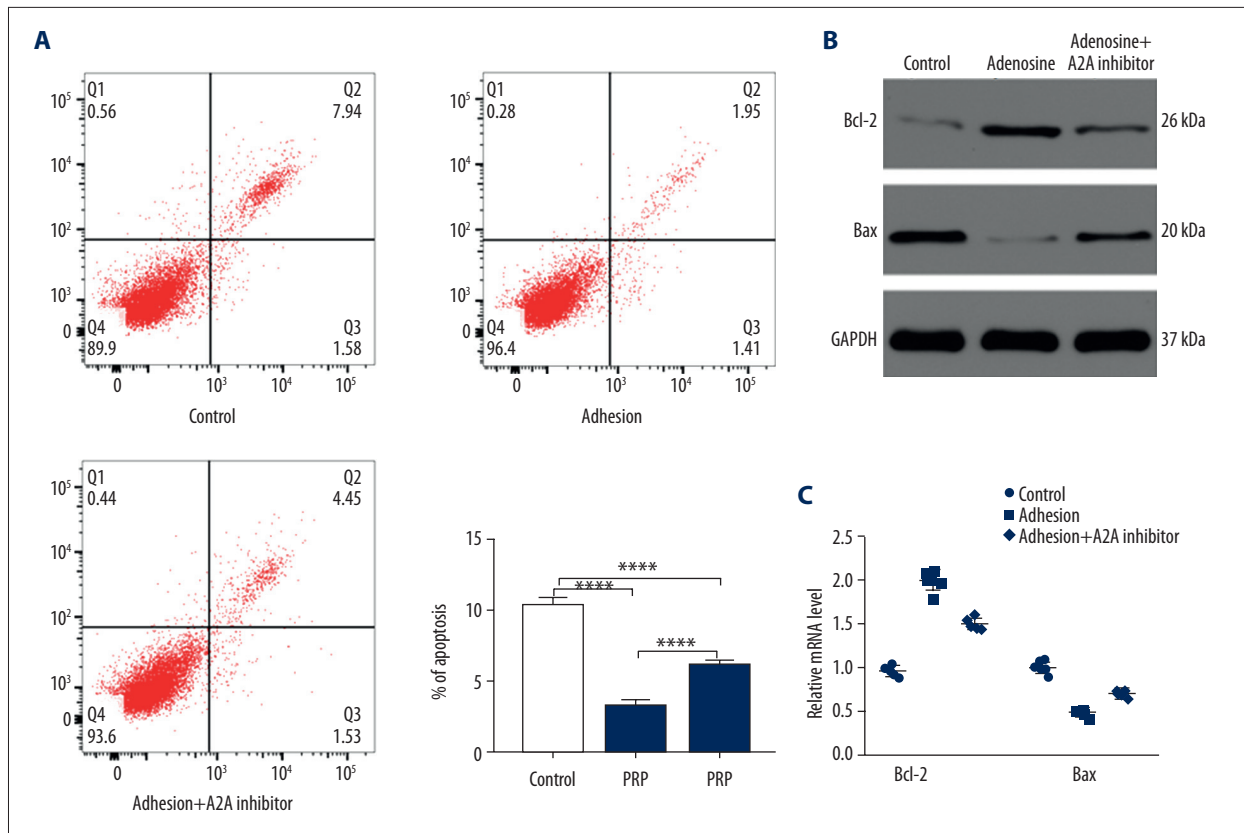


Figure 4. Adenosine inhibits fibroblast apoptosis via A2A receptor. (A) The apoptosis rate of fibroblasts among the 3 groups was measured by flow cytometry. (B) The levels of Bcl-2 and Bax were measured by western blot analysis. (C) qRT-PCR analysis was applied to detect the expression of Bcl-2 and Bax in control and PRP groups. * $P < 0.05$, **** $P < 0.0001$. PRP – platelet-rich plasma; qR-PCR – quantitative real-time polymerase chain reaction.

we treated fibroblasts with PBS, adenosine and adenosine+A2A receptor inhibitor group. Flow cytometry was used to assess the proliferation of fibroblasts among the 3 groups. The results showed that adenosine promoted cell proliferation that could be prevented through the administration of the A2A inhibitor (Figure 3B, 3C). The levels of cyclin D1 and cyclin D3 were measured by western blot (Figure 3D) and qRT-PCR (Figure 3E) and were consistent with the flow cytometry data.

Adenosine suppresses fibroblast apoptosis *in vitro*

Fibroblasts were treated with PBS, adenosine, and adenosine+A2A receptor inhibitor, and apoptosis rate were assessed by flow cytometry (Figure 4A). Our results showed that adenosine inhibits apoptosis, with the beneficial effects impaired by A2A receptor inhibition. In addition, the decreased levels of Bcl-2 and increased expression of Bax in the adenosine+A2A receptor inhibitor groups suggested that A2A receptor inhibitor treatment promotes cell apoptosis (Figure 4B, 4C). Taken together, these results indicated that adenosine significantly suppressed fibroblast apoptosis, an effect that could be alleviated by blocking the A2A receptor.

Besides, our data showed that the beneficial effect of PRP on fibroblasts could be partly impaired by A2A receptor, as evidenced by the inhibited proliferative ability and higher apoptosis rate in the PRP+A2A receptor group when compared to the PRP group (Figure 5). These data suggested that adenosine is critical in PRP-induced fibroblast proliferation.

sNAG hydrogel combined with PRP promote tissue regeneration *in vivo*

We next assessed the ability of sNAG hydrogels loaded with PRP to influence wound healing. We generated full-thickness cutaneous wounds on the backs of rats, and locally injected PBS, sNAG hydrogel, PRP, or sNAG hydrogel loaded with PRP onto the wound sites. As shown in Figure 6A and 6B, significantly faster wound closure rate was observed for sNAG hydrogels loaded with PRP. Furthermore, H&E staining suggested that rats treated with sNAG hydrogels loaded with PRP had smaller and shallower scars (Figure 6C, 6D). The Ki67 staining results showed that the proliferative rate of cells on wound was significantly higher in the sNAG+PRP group compared to the other 3 groups (Figure 6E). Together these findings revealed

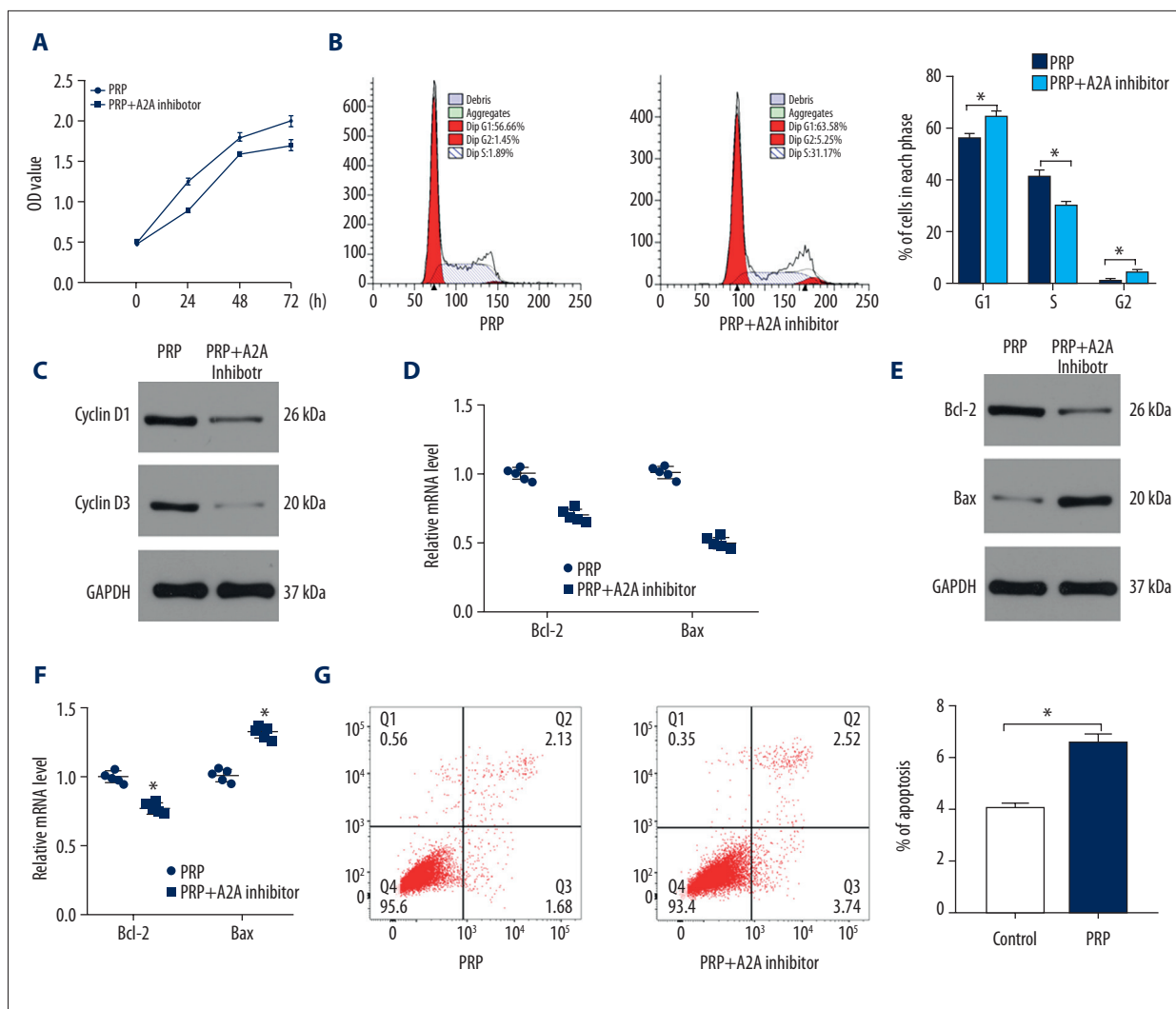


Figure 5. The beneficial effect of PRP on fibroblast function was partly attributed to adenosine. **(A, B)** CCK-8 assay and flow cytometry was used to evaluate the proliferation of fibroblasts. **(C, D)** The expression level of cyclin D1 and cyclin D3 was assessed by western blot and qRT-PCR. **(E–G)** The apoptosis of fibroblasts among the 2 groups was measured by western blot, qRT-PCR, and flow cytometry. * $P < 0.05$. PRP – platelet-rich plasma; CCK-8 – Cell Counting Kit-8; qR-PCR – quantitative real-time polymerase chain reaction.

that sNAG hydrogels loaded with PRP could promote *in vivo* wound healing.

Discussion

Appropriate concentration of PRP is vital for tissue healing. Studies have proposed that the platelet concentration most conducive to tissue healing is $1.5\text{--}3.0 \times 10^6/\mu\text{L}$, which is about 3-fold to 8-fold higher than the physiological concentration of platelets in whole blood [16]. Furthermore, recent studies have indicated that the immediate use of platelets after the inflammatory phase has the greatest effects on tissue healing [17]. It is suggested that the early use of PRP without delay

is more important than the number of platelets it contains [18]. However, concerns regarding the extraction process of autogenous PRP, such as phlebitis, infection, and anemia also exist [19]. It is therefore necessary to identify drug carriers that can support PRP and promote safe drug release.

SAPNS represents an advancement in biological materials, due to its ability to absorb moisture and insoluble 3-dimensional polymer hydrogels. Currently, sNAG hydrogels have been used in clinical practice as biological scaffolds [20,21]. Recent studies have reported that hydrogels can be encapsulated mesoporous silicon coated gold nanoshells as the only drug transporter [22], achieving outstanding clinical efficacy. Biodegradable hydrogel-loaded drugs have now been

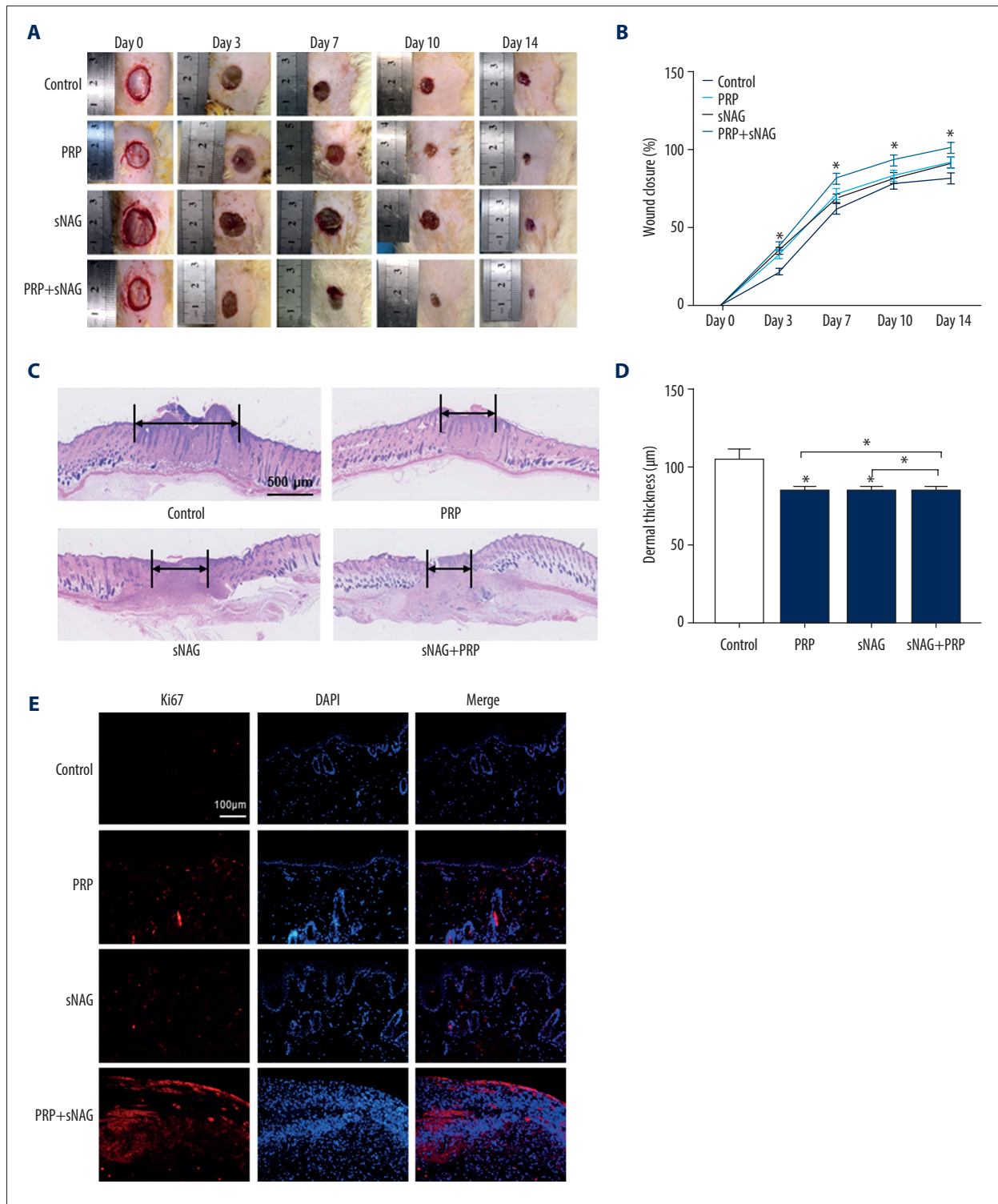


Figure 6. The effect of hydrogel loaded with PRP on wound healing *in vivo*. **(A)** Rat models were divided into 4 groups according different treatments. Gross view of the wounds on day 0, 3, 5, 7, 10, and 14 post-injury. **(B)** The closure rate of the wounds among the 4 groups (n=6). **(C)** H&E staining of the regenerative scars of the wounds (n=6). **(D)** The dermal thickness of the wounds (n=6). **(E)** The Ki67 staining of the wounds. * $P < 0.05$. PRP – platelet-rich plasma; H&E – hematoxylin-eosin.

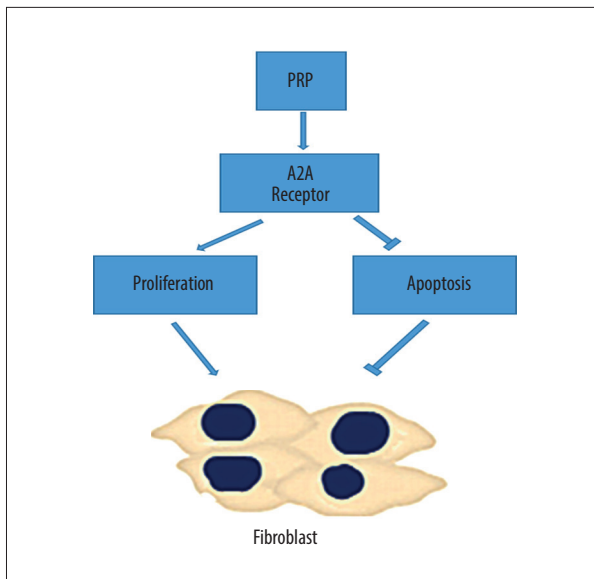


Figure 7. PRP induce proliferation and suppress apoptosis of fibroblasts via activation A2A receptors of adenosine. PRP – platelet-rich plasma.

synthesized which when injected under the skin, provide long-term immunity [23].

In the present research, we demonstrated that PRP can promote fibroblasts proliferation and inhibits apoptosis via activation of

References:

- Gurtner GC, Werner S, Barrandon Y et al: Wound repair and regeneration. *Nature*, 2008; 453(7193): 314–21
- Kirsner RS: The Wound Healing Society chronic wound ulcer healing guidelines update of the 2006 guidelines – blending old with new. *Wound Repair Regen*, 2016; 24(1): 110–11
- Gottrup FA: Specialized wound-healing center concept: importance of a multidisciplinary department structure and surgical treatment facilities in the treatment of chronic wounds. *Am J Surg*, 2004; 187(5A): 385–435
- Wicke C, Bachinger A, Coerper S et al: Aging influences wound healing in patients with chronic lower extremity wounds treated in a specialized Wound Care Center. *Wound Repair Regen*, 2009; 17(1): 25–33
- Jarbrink K, Ni G, Sonnergren H et al: Prevalence and incidence of chronic wounds and related complications: A protocol for a systematic review. *Syst Rev*, 2016; 5(1): 152
- Annunziata M, Oliva A, Buonaiuto C et al: *In vitro* cell-type specific biological response of human periodontally related cells to platelet-rich plasma. *J Periodont Res*, 2005; 40: 489–95
- Miroshnichenko S, Timofeeva V, Permykova E et al: Plasma-coated polycaprolactone nanofibers with covalently bonded platelet-rich plasma enhance adhesion and growth of human fibroblasts. *Nanomaterials (Basel)*, 2019; 9: 637
- Huber SC, Junior JLRC, Silva LQ et al: Freeze-dried versus fresh platelet-rich plasma in acute wound healing of an animal model. *Regen Med*, 2019; 14: 525–34
- Liu F, Xu HY, Huang H: A novel kartogenin-platelet-rich plasma gel enhances chondrogenesis of bone marrow mesenchymal stem cells *in vitro* and promotes wounded meniscus healing *in vivo*. *Stem Cell Res Ther*, 2019; 10: 201
- Mitek T, Nagraba Ł, Mitek T et al: Autologous platelet-rich plasma reduces healing time of chronic venous leg ulcers: A prospective observational study. *Adv Exp Med Biol*, 2019; 1176: 109–17
- Cui H, Webber MJ, Stupp SI: Self-assembly of peptide amphiphiles: From molecules to nanostructures to biomaterials. *Biopolymers*, 2010; 94(1): 1–18
- Bulut S, Erkal TS, Toksoz S et al: Slow release and delivery of antisense oligonucleotide drug by self-assembled peptide amphiphile nanofibers. *Biomacromolecules*, 2011; 12(8): 3007–14
- Bradshaw M, Ho D, Fear MW et al: Designer self-assembling hydrogel scaffolds can impact skin cell proliferation and migration. *Sci Rep*, 2014; 4: 6903
- Paladini F, Meikle ST, Cooper IR et al: Silver-doped self-assembling di-phenylalanine hydrogels as wound dressing biomaterials. *J Mater Sci Mater Med*, 2013; 24: 2461–72
- Kido T, Schubert S, Hatakeyama S et al: Expression of a Y-located human proto-oncogene TOPY in a transgenic mouse model of prostate cancer. *Cell Bosco*, 2014; 4: 9
- Zhang H, Zeng H, Primages A et al: Programmable responsive hydrogels inspired by classical conditioning algorithm. *Nat Commun*, 2019; 10: 3267
- Bahcecioglu G, Bilgen B, Hasirci N et al: Anatomical meniscus construct with zone specific biochemical composition and structural organization. *Biomaterials*, 2019; 218: 119361
- Ateia M, Arifuzzaman MD, Pellizzeri S et al: Cationic polymer for selective removal of GenX and short-chain PFAS from surface waters and wastewaters at ng/L levels. *Water Res*, 2019; 163: 114874
- Saleh B, Dhaliwal HK, Portillo-Lara R et al: Local immunomodulation using an adhesive hydrogel loaded with miRNA-laden nanoparticles promotes wound healing. *Small*, 2019; 15(36): e1902232
- Xu Q, Zhao S, Deng L et al: A NIR-II light responsive hydrogel based on 2D engineered tungsten nitride nanosheets for multimode chemo/photothermal therapy. *Chem Commun (Camb)*, 2019; 55(64): 9471–74

adenosine A2A receptor, and thereby promoting wound healing *in vivo*. *In vivo*, we synthesized a sNAG hydrogel composed of isoleucine-lysine-valine-alanine-valine and arginine-glycine-aspartic acid (RGD). The sNAG hydrogel could be a good carrier to PRP. In the present study, we performed sNAG hydrogel encapsulated PRP to observe the effect on wound healing. Through *in vivo* study, we found that PRP+SNPAS hydrogel-treated rats obtained the fastest healing rate as relative to other groups. Furthermore, H&E staining indicated that the combination of PRP and SNPAS hydrogel together promote wound disclosure, which demonstrated that the application of PRP and SNPAS hydrogel can be coordinated to accelerates wound healing process.

Conclusions

Our results indicated that the combination of PRP and SNPAS hydrogels promotes wound healing through increased proliferation and the prevention of fibroblasts apoptosis through adenosine A2A receptor activation (Figure 7). *In vivo* and *in vitro* studies are now required to define the detailed molecular mechanisms by which PRP accelerates wound healing.

Conflict of interest

None.

21. Murphy SV, Skardal A, Nelson RA et al: Amnion membrane hydrogel and amnion membrane powder accelerate wound healing in a full thickness porcine skin wound model. *Stem Cells Transl Med*, 2019 [Epub ahead of print]
22. Kim BS, Chen YT, Srinoi P et al: Hydrogel-encapsulated mesoporous silica-coated gold nanoshells for smart drug delivery. *Int J Mol Sci*, 2019; 20(14): pii: E3422
23. Lee ALZ, Yang C, Gao SJ et al: Subcutaneous vaccination using injectable biodegradable hydrogels for long-term immune response. *Nanomedicine* 2019, 21: 102056